

# An Input Observer-based Stiffness Estimation Approach for Flexible Robot Joints

Adriano Fagiolini<sup>1</sup>, Maja Trumić<sup>2</sup>, and Kosta Jovanović<sup>3</sup>

**Abstract**—This paper addresses the stiffness estimation problem for flexible robot joints, driven by variable stiffness actuators in antagonistic setups. Due to the difficulties of achieving consistent production of these actuators and the time-varying nature of their internal flexible elements, which are subject to plastic deformation over time, it is currently a challenge to precisely determine the total flexibility torque applied to a robot’s joint and the corresponding joint stiffness. Herein, by considering the flexibility torque acting on each motor as an unknown signal and building upon Unknown Input Observer theory, a solution for electrically-driven actuators is proposed, which consists of a linear estimator requiring only knowledge about the positions of the joints and the motors as well as the drive’s dynamic parameters. Beyond its linearity advantage, another appealing feature of the solution is the lack of need for torque and velocity sensors. The presented approach is first verified via simulations and then successfully tested on an experimental setup, comprising bidirectional antagonistic variable stiffness actuators.

**Index Terms**—Flexible Robots, Natural Machine Motion, Calibration and Identification, Failure Detection and Recovery.

## I. INTRODUCTION

SOFT robots have been brought into the limelight as cutting-edge technology, primarily with the vision of enabling humans a harmless physical interaction with robots [1]. Practically divided into soft-bodied and articulated soft robots, whose dynamics have just recently been shown to match under suitable assumptions [2], they are intrinsically endowed with the capacity of dynamically modulating elasticity while moving, which opens many opportunities for the amelioration of various life aspects [3], [4]. For articulated soft robots, i.e. robots with elasticity concentrated mostly at their joints, the achievement of human-like abilities, such as dexterity and robustness, relies on the availability of so-called Variable Stiffness Actuators (VSA). Most attention is nowadays turned to electrically-driven VSAs, that enable accurate position and velocity control, while also allowing online compliance adjustment [5]. These actuators are generally preferred to their pneumatic and hydraulic counterparts for their greater compactness,

Manuscript received: September, 10, 2019; Revised December, 14, 2019; Accepted January, 9, 2020.

This paper was recommended for publication by Editor Kyu-Jin Cho upon evaluation of the Associate Editor and Reviewers’ comments. This work was supported by the University of Belgrade with project TR35003.

<sup>1</sup>A. Fagiolini is with the Department of Engineering, University of Palermo, Italy, fagiolini@unipa.it

<sup>2</sup>M. Trumić is with the Department of Engineering, University of Palermo, Italy, and with the School of Electrical Engineering, University of Belgrade, Serbia, maja.trumic@unipa.it

<sup>3</sup>K. Jovanović is with the School of Electrical Engineering, University of Belgrade, Serbia, kostaj@etf.rs

Digital Object Identifier (DOI): see top of this page.

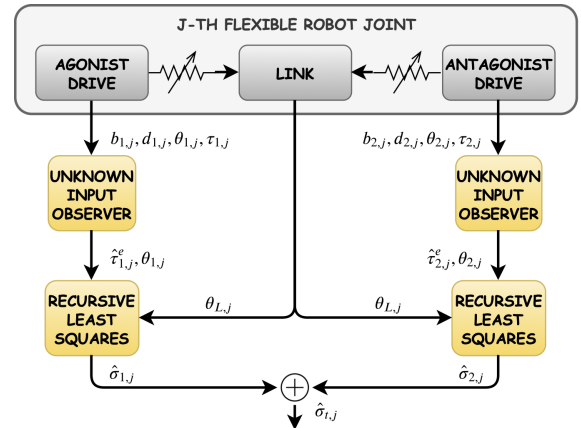


Fig. 1. Block scheme of the algorithm for estimation of stiffness in flexible robot joints, actuated by antagonistic VSA.

for being more silent, and not requiring external devices, such as air compressors. Systems such as Kuka’s lightweight robot, endowed with active compliance control [6], and other novel cost-effective, open-source solutions, including e.g. the products by Natural Machine Motion Initiative [7], are now emerging on the market, all sharing the common aspiration to empower faster development of this field.

The advantages of variable stiffness actuation arise in various tasks, such as when performing cyclic movements for dribbling a ball [8], during explosive actions of autonomous hammering [9], for safe human-robot interaction [10], and indeed in many others. However, the key enabler of these benefits is in fact the capacity of effectively controlling the stiffness, at the joint or end-effector level. Different solutions of closed-loop stiffness control have already been explored, including feedback linearization [11], backstepping [12], adaptive control [13], LQR-based gain scheduling [14], all with the assumption that an accurate and reliable stiffness estimate is available. On the contrary, so far, since stiffness is not measurable, its regulation is mostly done in open-loop, by leveraging on model-based computation. In this case, one can either do an extensive experimentation and identification, in order to obtain an accurate stiffness model, or can rely on datasheets from the manufacturers. Even in the case that the provided datasheets are initially reliable, the continuous wear induced by the impact of forces, acting on the elastic elements, the temperature drifts, and the torque hysteresis eventually result in additional inaccuracies [15]. This motivates the development of online stiffness estimators, which is the goal of the current paper.

**Previous work.** The main concept behind the stiffness estimation problem is that of finding the first derivative of the flexibility torque with respect to the flexible transmission. Pioneering results focused on estimating Cartesian stiffness [16], under the assumption that the robot’s end-effector is in contact with the environment. Moreover, joint stiffness estimation appears to be more convenient as it covers a general case when the contact between robot and environment can also happen sideways. To this regard, the online non-parametric stiffness estimator presented in [17] is able to identify stiffness from the link side, without needing any information of the actuating drive. Beyond the need to compute the time derivative of torque sensor from possibly noisy data, the practical applicability of such approaches remains challenging also because the state observability property is lost when the robot’s link is in steady state.

A different perspective to the challenging problem of online stiffness estimation, which uses also measurements from the motor side, is the one offered by the promising research line of the work in [18]. In the solution therein proposed, joint stiffness estimator is achieved via a two-phase process: first, an estimate of the flexibility torque applied to each motor is obtained by using residuals, and then a Recursive Least Square (RLS) algorithm is used to determine torque and stiffness approximations, which are parameterized with respect to the flexible transmission. The approach requires knowledge of the motor speed, which is estimated through a Modified Kinetic Kalman Filter (MKKF), whose parameters have to be properly tuned [19]. Another interesting method estimating instead stiffness in a direct way, and not requiring the computation of time derivatives, is the one proposed in [20], which uses so-called modulating functions. While the approach is advantageous as it provides a proof of the estimation error convergence, it requires an a-priori choice of the RLS algorithm parameters and of the integration window length, one of the modulating function parameter.

**Contributions.** This paper proposes an alternative technique for the estimation of stiffness and flexibility torque in robot joints. Similarly to above-mentioned methods, the challenge is tackled here from the motor side, but here, as a pivotal point of the strategy, by considering the flexibility torque signal as an unknown input of the linear motor model. With this regard, Unknown Input Observers (UIO) are useful tools that have mainly been used for detecting system failures, by achieving correct state estimation independently of the unknown inputs. In this case, however, we focus on estimating the unknown input, which is a nonlinear time-variant function of our system variables. Among the input-observer categories studied in the literature, so-called “delayed” input-observers [21], [22], [23] are preferable for our problem as they provide more information about the system. Indeed, thanks to the use of multiple output values, collected over consecutive sampling times, they are capable of estimating both the system’s states and inputs, with a constant and predetermined delay, and they involve looser existence conditions for the realization of the input-observer. This leads us to the appealing feature of being able to asymptotically reconstruct the unknown flexibility torque, without velocity sensor measurements, otherwise necessary

with the observer obtained via the zero-delay approach [24]. Finally, compared to the approach in [25], the one in [21], which we rely on, leads to a smaller state space of the observer. Once flexibility torque is estimated via the UIO, the stiffness is straightforwardly determined by the RLS.

Furthermore, compared to the solution presented in [17], approaching the problem from the link side, the current approach avoids the known observability issue and does not require the installation of torque sensors, as it considers the problem from the motor side. Moreover, compared to the method presented in [19], the present one requires no tuning of a Kalman Filter, thanks to the capacity of the UIO to simultaneously estimate velocity of motors and flexibility torque. However, similarly to [19], our approach estimates both joint stiffness and flexibility torque, which is useful for model-based control laws, but on the other hand it lacks the proof of stiffness convergence which is provided instead in [20]. Finally, while the approach in [20] requires a suitable tuning of the integration window length depending on the signal to be elaborated, our UIO-based approach involves matrices that are a-priori determined and thus independent of the signal rate. As a consequence, the UIO output alone tends to be more susceptible to noise, but the concurrently running RLS algorithm is capable of successfully compensating for it. It is also worth mentioning that, thanks to the decentralized structure of motor dynamic equations, our method can be applied for the stiffness estimation in flexible joints of robots with multiple degrees of freedom, joints driven by different VSA configurations, and, consequently, for Cartesian stiffness estimation based on joints’ positions and stiffnesses.

The paper is organized as follows. Section II introduces the model of elastic joint driven by variable stiffness actuator in antagonistic setup. The UIO existence conditions and the design procedures are presented in Section III, thus leading to the development of our flexibility torque estimator. Section IV and V present a simulative evaluation of the solution and final experimental results, respectively. Section VI summarizes the achievements and presents a final discussion.

## II. PROBLEM STATEMENT

Consider an  $n$  degree-of-freedom robot with flexible joints driven by electrical VSAs in agonist-antagonistic configurations. More precisely, each joint of the robot is actuated by a couple of DC motors, which are connected to the joint via tendons as in Fig. 1. By changing the internal motors’ positions, it is possible to vary both joint’s position (if motors rotate in the same direction) and stiffness (when motors rotate in opposite directions). As described in [26], the robot’s dynamical model can be written as follows:

$$\begin{aligned} B_L \ddot{\theta}_L + h_L(\theta_L, \dot{\theta}_L) + \tau_t^e(\phi_1, \phi_2) + g(\theta_L) &= \tau_{\text{ext}}, \\ B_1 \ddot{\theta}_1 + D_1 \dot{\theta}_1 - \tau_1^e(\phi_1) &= \tau_1, \\ B_2 \ddot{\theta}_2 + D_2 \dot{\theta}_2 - \tau_2^e(\phi_2) &= \tau_2, \end{aligned} \quad (1)$$

where  $\theta_L \in \mathbb{R}^n$  is the link angle vector,  $\tau_t^e$  is the total flexibility torque vector, and where  $\theta_i \in \mathbb{R}^n$ ,  $\tau_i^e$ , and  $\tau_i$  are the motor position vectors, flexibility torque vectors, and commanded torque vectors, respectively, for the agonistic

( $i = 1$ ) and antagonistic ( $i = 2$ ) motor. Moreover,  $B_L$  is the robot link inertia matrix,  $h_L(\cdot)$  includes Coriolis, viscous friction, and centrifugal terms, and  $g(\cdot)$  is a vector of gravity forces; matrices  $B_i = \text{diag}(b_{i,j})$  and  $D_i = \text{diag}(d_{i,j})$  contain motor's inertia and damping coefficients, respectively; finally,  $\tau_{ext}$  is the external torque, assumed to be null in the remainder of the work.

Furthermore, having denoted with  $\phi_i = \theta_L - \theta_i$  the transmission deflection vectors of the agonistic and antagonistic motor's transmission, the total flexibility torque  $\tau_t^e$ , in the first equation of the model, is given by

$$\tau_t^e = \tau_1^e(\phi_1) + \tau_2^e(\phi_2). \quad (2)$$

The above element-wise dependency on the transmission deflection, i.e. the fact that for the  $j$ -th joint  $\tau_{i,j}^e = \tau_{i,j}^e(\phi_{i,j})$ , along with the diagonal form of the motor's inertia and damping matrices, justifies a decentralized viewpoint of motor's dynamics. It can be assumed that the flexibility torque is an odd function, meaning that compression and extension have the same effect on transmission behavior. The components  $\sigma_{i,j}$  of the stiffness vector  $\sigma_i$  of each transmission are by definition

$$\sigma_{i,j}(\phi_{i,j}) = \frac{\partial \tau_{i,j}^e}{\partial \phi_{i,j}}(\phi_{i,j}),$$

leading to the total joint stiffness

$$\sigma_t = \sigma_1(\phi_1) + \sigma_2(\phi_2). \quad (3)$$

Finally, for the  $i$ -th motor of the  $j$ -th joint, one can define the state vector  $x_{i,j} = (\theta_{i,j}, \dot{\theta}_{i,j})^T$ , the input vector  $u_{i,j} = (\tau_{i,j}^e, \tau_{i,j})^T$ , and the output vector  $y_{i,j} = (\theta_{i,j}, \tau_{i,j})^T$ . The motor's dynamics then reads

$$\begin{aligned} \dot{x}_{i,j} &= A_c x_{i,j} + B_c u_{i,j}, \\ y_{i,j} &= C x_{i,j} + D u_{i,j}, \end{aligned} \quad (4)$$

with

$$\begin{aligned} A_c &= \begin{pmatrix} 0 & 1 \\ 0 & -d_{i,j}/b_{i,j} \end{pmatrix}, \quad B_c = \begin{pmatrix} 0 & 0 \\ 1/b_{i,j} & 1/b_{i,j} \end{pmatrix}, \\ C &= \begin{pmatrix} 1 & 0 \\ 0 & 0 \end{pmatrix}, \quad D = \begin{pmatrix} 0 & 0 \\ 0 & 1 \end{pmatrix}. \end{aligned}$$

The aim is thus finding a solution for estimating the state and the unknown input for each motor, which will also justify the choice of output and feed-through matrices made above.

### III. THE PROPOSED STIFFNESS ESTIMATION APPROACH

This section thoroughly presents the design procedure of a UIO. First, a general framework for the observation of a linear system with unknown inputs is recalled from [21]; then, the properties of a DC motor system are explored and the appropriate UIO is designed; finally, an RLS algorithm is illustrated for stiffness estimation.

#### A. Theoretical Framework

The use of a so-called UIO filter has the advantage of simultaneously allowing state estimation and unknown input reconstruction. The main concept capitalizes on the equivalence between linear system's invertibility and unknown input observability, which has been explored in [27], [28]. Let us consider a linear, time-invariant, discrete-time system in a general form

$$\begin{aligned} X_{k+1} &= A X_k + B U_k, \\ Y_k &= C X_k + D U_k, \end{aligned} \quad (5)$$

where  $X_k \in \mathbb{R}^n$  is a state vector,  $U_k \in \mathbb{R}^m$  contains the unknown inputs,  $Y_k \in \mathbb{R}^p$  is an output vector,  $A$ ,  $B$ ,  $C$ , and  $D$  are suitable matrices. Given a time delay  $L$ , the history of the system's output  $\mathbb{Y}_k^L = (Y_k^T, \dots, Y_{k+L}^T)^T$ , can be obtained from [21] as

$$\mathbb{Y}_k^L = O^L X_k + \mathbb{H}^L U_k^L, \quad (6)$$

where  $U_k^L = (U_k^T, \dots, U_{k+L}^T)^T$  is the input history, and

$$\begin{aligned} O^L &= (C^T, (CA)^T, (CA^2)^T, \dots, (CA^{L-1})^T)^T = \\ &= (C^T, (O^{L-1}A)^T)^T, \end{aligned}$$

and

$$\mathbb{H}^L = \begin{pmatrix} D & 0 & 0 & 0 & \dots & 0 \\ CB & D & 0 & 0 & \dots & 0 \\ CAB & CB & D & 0 & \dots & 0 \\ \vdots & \vdots & \vdots & \vdots & \ddots & \vdots \\ CA^{L-1}B & CA^{L-2}B & \dots & \dots & CB & D \end{pmatrix}.$$

are the  $L$ -step observability and invertibility matrices, respectively. A discrete-time linear UIO is given by

$$\begin{aligned} \hat{X}_{k+1} &= E \hat{X}_k + F \mathbb{Y}_k^L, \\ \hat{U}_k &= G \begin{pmatrix} \hat{X}_{k+1} - A \hat{X}_k \\ Y_k - C \hat{X}_k \end{pmatrix}, \end{aligned} \quad (7)$$

where  $E$  and  $F$  are observer matrices of suitable dimensions, being designed such that  $\hat{X}_k \rightarrow X_k$  and  $\hat{U}_k \rightarrow U_k$ , and where  $G = (B^T, D^T)^T \dagger$  is an input decoupling matrix, with full column rank, and  $P \dagger$  is the pseudo-inverse of a matrix  $P$ .

#### B. System properties

Given a sampling time  $T$ , by applying Euler's method, the motor dynamics in 4 can be converted to a discrete-time form equivalent to 5, where  $A = I_2 + TA_c$ ,  $B = TB_c$ , and  $I_d$  is an identity matrix of size  $d$ . It is straightforward to conclude that the system is fully observable. However, regarding the existence conditions of a UIO, it is important to additionally examine the invertibility and strong observability of the system through the following:

*Proposition 1 (System Invertibility):* A linear dynamic system with state form as in Eq. 5, with state vector  $X_k \in \mathbb{R}^n$  and  $U_k \in \mathbb{R}^m$ , is invertible with delay  $L$  if, and only if, the condition  $\text{rank}(\mathbb{H}^L) = m + \text{rank}(\mathbb{H}^{L-1})$  is satisfied for some  $L \leq n$ , where  $\text{rank}(\mathbb{H}^{-1}) = 0$  by definition.

According to Prop. 1, the sought delay, allowing the unknown input reconstruction, is  $L = 2$ , for which the observability and invertibility matrices are the following:

$$O^2 = \begin{pmatrix} C \\ CA \\ CA^2 \end{pmatrix} = \begin{pmatrix} 1 & 0 & 1 & 0 & 1 & 0 \\ 0 & 0 & T & 0 & T(2 + \beta T) & 0 \end{pmatrix}^T,$$

$$\mathbb{H}^2 = \begin{pmatrix} D & 0 & 0 \\ CB & D & 0 \\ CAB & CB & D \end{pmatrix} = \begin{pmatrix} 0 & 0 & 0 & 0 & 0 & 0 \\ 0 & 1 & 0 & 0 & 0 & 0 \\ 0 & 0 & 0 & 0 & 0 & 0 \\ 0 & 0 & 0 & 1 & 0 & 0 \\ \gamma & \gamma & 0 & 0 & 0 & 0 \\ 0 & 0 & 0 & 0 & 0 & 1 \end{pmatrix},$$

where  $\beta = -\frac{d_{i,j}}{b_{i,j}}$  and  $\gamma = T^2/b_{i,j}$ . Moreover, as the system output in Eq. 6 depends also on the initial state, whose knowledge can be approximate, it is useful to check also the system's strong observability according to the following:

*Definition 1:* A discrete-time system as in Eq.5 is *strongly observable* if, for any initial state  $X_0$  and any unknown input sequence  $U_0, U_1, \dots$ , there exists a positive integer  $L$  such that  $X_0$  can be recovered from the output sequence  $Y_0, Y_1, \dots$

*Proposition 2 (Strong Observability):* A discrete-time system in Eq. 5 where  $X_k \in \mathbb{R}^n$  is strongly observable if, and only if, for some  $L \leq n$ , it holds

$$\text{rank}([O^L, \mathbb{H}^L]) = n + \text{rank}(\mathbb{H}^L).$$

The strong observability condition is satisfied, in our case, for a delay  $L = 2$ , which allows us to conclude that a two-sample delay is necessary and sufficient for observing unknown inputs.

### C. Design procedure

We are now able to provide the following result:

*Theorem 1 (Stiffness Estimator):* Given the motor's dynamic model in Eq. 5, a UIO system estimating its state and its unknown inputs, including the local flexibility torque, is described by the state-form in Eq. 7, where  $L = 2$  and

$$E = \begin{pmatrix} 1 & T \\ -\frac{1}{T} & -1 \end{pmatrix}, F = \begin{pmatrix} 0 & 0 & 0 & 0 \\ 0 & 0 & \frac{T}{b_{i,j}} & \frac{T}{b_{i,j}} \end{pmatrix},$$

$$G = \begin{pmatrix} 0 & -b_{i,j} & 0 & 1 \\ 0 & 0 & 0 & 1 \end{pmatrix}.$$

*Proof 1:* The conditions for the observer's stability are examined by driving the estimation error to zero, whose dynamics is:

$$\begin{aligned} e_{k+1} &= \hat{X}_{k+1} - X_{k+1} = \\ &= E \hat{X}_k + F \mathbb{Y}_k^L - A X_k - B U_k = \\ &= E e_k + F \mathbb{Y}_k^L + (E - A) X_k - B U_k = \\ &= E e_k + (E - A + F O^L) X_k \\ &+ F \mathbb{H}^L U_k^L - B U_k, \end{aligned}$$

which leads to the conclusion that  $E$  has to be a stable matrix and  $F$  has to be chosen so that following is satisfied:

$$F \mathbb{H}^L = (B \ 0 \ \dots \ 0), \quad (8a)$$

$$E = A - F O^L. \quad (8b)$$

The condition for the existence of matrix  $F$  is equivalent to the one given in Prop. 1, while the matrix is obtained by following the design procedure described in [21], [23], shortly presented below.

First, let us take a look at the first Eq. 8a which is also called input-decoupling equation, as it decouples input from the estimation error. The matrix  $F$  can be expressed as  $F = \hat{F}_1 N = (\hat{F}_1, \hat{F}_2) N$ , where  $N$  is chosen such that  $N \mathbb{H}^L = \begin{pmatrix} 0 & 0 \\ I_m & 0 \end{pmatrix}$ . This straightforwardly leads to the conclusion that  $\hat{F}_2 = B$ . Moving now on to the state-decoupling equation 8b, named after property to decouple states and estimation error, the design degree-of-freedom of matrix  $\hat{F}_1$  is used to suitably allocate eigenvalues of  $E$ , in order to keep it stable. If any desired eigenvalue position is given, robust pole placement procedures such as the one described in [29] are recommended. In the present case, all eigenvalues of  $E$  are already in zero, thus realizing a dead-beat observer with finite-time convergence, and hence matrix  $\hat{F}_1$  is chosen to be the null matrix. This finally yields the relation presented in the theorem.

### D. Recursive Least Square Algorithm

Once the flexibility torque has been estimated by the UIO, an RLS algorithm is used to determine the coefficients of a  $\kappa$ -th order parametric approximation of such torque with respect to flexible transmission, being  $\hat{\tau}_{i,j}^e = \Phi_{i,j} \Pi_{i,j}$ , where the quantities

$$\Phi_{i,j} = (\phi_{i,j}, \phi_{i,j}^3, \dots, \phi_{i,j}^{2\kappa+1}),$$

$$\Pi_{i,j} = (\pi_{i,j,1}, \pi_{i,j,2}, \dots, \pi_{i,j,\kappa})^T,$$

are a regressor matrix, comprising only odd powers of the transmission deflection as we assumed flexibility torque oddness, and the corresponding vector of unknown parameters, respectively. The order  $\kappa$  is chosen so that the main features are captured and simultaneously the estimation is denoised. Having denoted with  $\hat{\Pi}_{i,j}[k] = (\hat{\pi}_{i,j,1}[k], \dots, \hat{\pi}_{i,j,\kappa}[k])^T$  the parameter vector estimated at the  $k$ -th step, the following RLS algorithm proposed in [30] can be used:

$$\begin{aligned} \epsilon_{i,j}[k] &= \hat{\tau}_{i,j}^e[k] - \Phi_{i,j}[k] \hat{\Pi}_{i,j}[k], \\ \rho_{i,j}[k] &= \Phi_{i,j}^T[k] P_{i,j}[k-1] \Phi_{i,j}[k], \\ K_{i,j}[k] &= (1 + \rho_{i,j}[k])^{-1} (P_{i,j}[k-1] \Phi_{i,j}[k]), \\ \hat{\Pi}_{i,j}[k] &= \hat{\Pi}_{i,j}[k-1] + K_{i,j}[k] \epsilon_{i,j}[k], \\ P_{i,j}[k] &= P_{i,j}[k-1] - K_{i,j}[k] \Phi_{i,j}^T[k] P_{i,j}[k-1], \end{aligned}$$

where  $P_{i,j}$  is the parameter covariance matrix. The algorithm is initialized with an a-priori assumption of parameters  $\hat{\Pi}_{i,j}[0]$  and a positive definite covariance matrix  $P_{i,j}[0]$ . Afterward, stiffness is calculated as a first derivative of the flexibility torque approximation:

$$\hat{\sigma}_{i,j} = \frac{\partial \hat{\tau}_{i,j}^e}{\partial \phi_{i,j}} = \frac{\partial \Phi_{i,j}}{\partial \phi_{i,j}} \hat{\Pi}_{i,j}.$$

## IV. SIMULATION VALIDATION

The proposed technique has first been validated in simulations on a two degree-of-freedom soft robot, with rotary joints

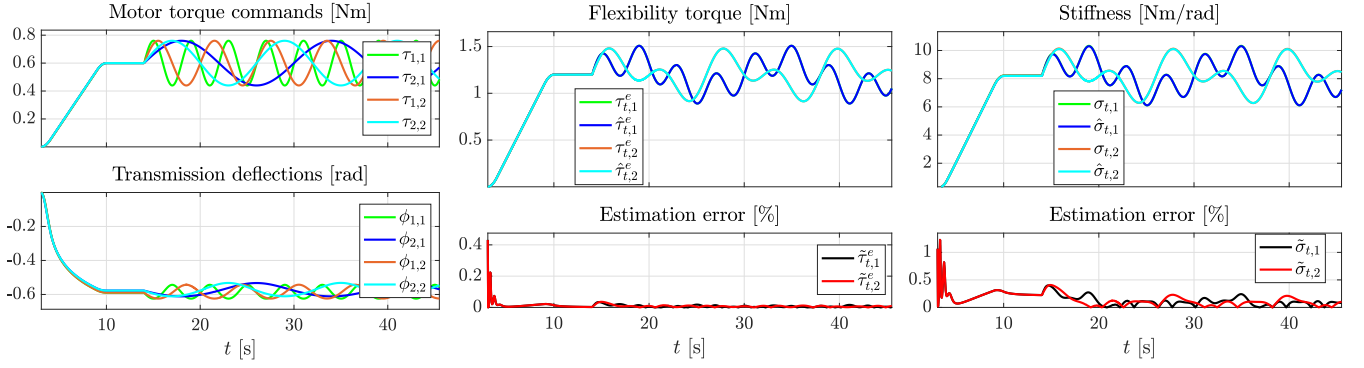


Fig. 2. Simulation run of a two degree-of-freedom flexible joint robot driven by antagonistic VSA. From left to right, commanded torques  $\tau_{i,j}$  applied to the motors and obtained transmission deflections  $\phi_{i,j}$ , estimated total flexibility torque  $\hat{\tau}_{t,j}^e$  for each joint and corresponding error percentage  $\tilde{\tau}_{t,j}^e = (\hat{\tau}_{t,j}^e - \tau_{t,j}^e)/\tau_{t,j}^e$ , and estimated stiffness  $\hat{\sigma}_{t,j}$  in each joint and error percentage  $\tilde{\sigma}_{t,j} = (\hat{\sigma}_{t,j} - \sigma_{t,j})/\sigma_{t,j}$ . Both flexibility torques and stiffnesses are estimated effectively with quite small relative error.

actuated by antagonistic VSAs, mounted in a vertical plane. The simulated actuators are *Qbmove Maker Pro* with servo DC motors provided by *qb-robotics*. According to the robot model in Eq. 1 and data-sheets [31], the flexibility torque generated by each drive and the corresponding stiffness are

$$\begin{aligned} \tau_{i,j}^e &= k_i \sinh(a_i(\theta_{L,j} - \theta_{i,j})), \\ \sigma_{i,j} &= a_i k_i \cosh(a_i(\theta_{L,j} - \theta_{i,j})), \end{aligned} \quad (9)$$

where  $a_i$  and  $k_i$  denote VSA string characteristic, assumed to be same for each joint. The total flexibility torque and stiffness of the joint are straightforwardly determined in compliance with Eq. 2 and 3. Nominal values for the stated VSA are  $b_{i,j} = 3 \cdot 10^{-6}$  [kgm<sup>2</sup>],  $d_{i,j} = 10^{-6}$  [Nms/rad],  $a_1 = 6.7328$  [Nm],  $k_1 = 0.0227$  1/rad,  $a_2 = 6.9602$  [Nm], and  $k_2 = 0.0216$  1/rad. Given the decentralized structure of motors' dynamics (cf. Sec. II) and the fact that motors have the same characteristics by construction, the local flexibility torque at every motor  $i$  can be estimated by a copy of the very same UIO, which is designed only once, with a delay  $L = 2$ . Moreover, the following Taylor expansion of the flexibility torque and the corresponding stiffness approximation are used:

$$\begin{aligned} \hat{\tau}_{i,j}^e &= \sum_{n=0}^3 (\theta_{L,j} - \theta_{i,j})^{2n+1} \pi_{i,j,n+1}, \\ \hat{\sigma}_{i,j} &= \sum_{n=0}^3 (2n+1) (\theta_{L,j} - \theta_{i,j})^{2n} \pi_{i,j,n+1}. \end{aligned}$$

Starting the RLS algorithm with complete lack of knowledge of the parameter values, i.e. with a null  $\hat{\Pi}_{i,j}[0]$ , and an initial covariance matrix  $P_{i,j}[0] = 10^8 I_4$ , the simulation, run with a sampling period of  $T = 10^{-3}$  [s], gives the results reported in Fig. 2 and Fig. 3. More precisely, Fig. 2 shows the commanded torques to drives, which are chosen to be sinusoidal with the same amplitude of 0.15 [Nm] and with different frequencies of 0.25 [Hz] for  $\tau_{1,1}$ , 0.06 [Hz] for  $\tau_{1,2}$ , 0.17 [Hz] for  $\tau_{2,1}$ , and 0.08 [Hz] for  $\tau_{2,2}$ , and corresponding deflections. The figure also reports the total flexibility torque and stiffness estimation via UIO and RLS algorithm, as well as the relative error of the estimation with respect to the reference models. It is apparent that the UIO accurately estimates the flexibility torque with a negligible delay of 2 milliseconds. Estimation errors of flexibility torque and joint stiffness of few percents appear only during an initial phase, when the parameters' convergence has not been achieved yet. Furthermore, it is

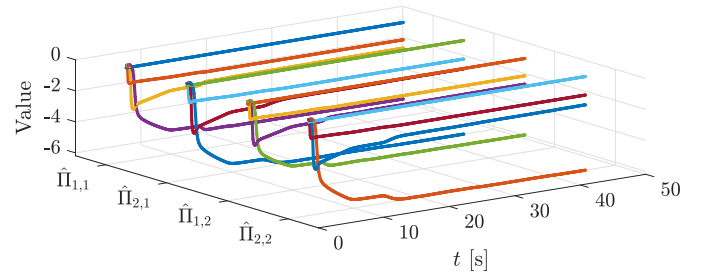


Fig. 3. Temporal evolution of the parameter vectors estimated via the RLS algorithm in Matlab/Simulink. Parameters rapidly converge and remain constant.

TABLE I  
EVALUATION CRITERIA FOR SIMULATED RESULTS

		MSE [Nm <sup>2</sup> /rad <sup>2</sup> ]	MSREP [%]
Stiffness estimation	1 <sup>st</sup> joint	$1.84 \cdot 10^{-7}$	$3.34 \cdot 10^{-7}$
	2 <sup>nd</sup> joint	$1.92 \cdot 10^{-7}$	$3.38 \cdot 10^{-7}$
Torque estimation	1 <sup>st</sup> joint	$1.49 \cdot 10^{-11}$	$2.85 \cdot 10^{-9}$
	2 <sup>nd</sup> joint	$1.62 \cdot 10^{-11}$	$2.84 \cdot 10^{-9}$

worth noticing that the estimation performance is not affected by the joints' dynamic coupling, which is in accordance with the result in [19], stating that the decentralized structure of motor dynamics allows the approach to be applied also to multiple degree-of-freedom robots. Moreover, Fig. 3 shows the estimated parameters' evolution over time. It is noticeable that, with rigid robot links as in our case, the robot's Cartesian stiffness can be straightforwardly calculated based on its well-known relation with joint stiffness [26]. Finally, Tab. I reports a summary of the estimation performance for both torque and stiffness in each joint. Given two sample sequences of a real signal  $\chi$  and an estimated signal  $\hat{\chi}$ , the Mean Square Error (MSE) and Mean Square Relative Error Percentage (MSREP) indices, used in the above table, are defined as follows:

$$\begin{aligned} \text{MSE} &= \frac{1}{n_2 - n_1 + 1} \sum_{n=n_1}^{n_2} (\chi(n) - \hat{\chi}(n))^2, \\ \text{MSREP} &= \frac{1}{n_2 - n_1 + 1} \sum_{n=n_1}^{n_2} (\chi(n) - \hat{\chi}(n))^2 / \chi^2(n), \end{aligned}$$

where  $n_1$  and  $n_2$  indicate the initial and final time interval.

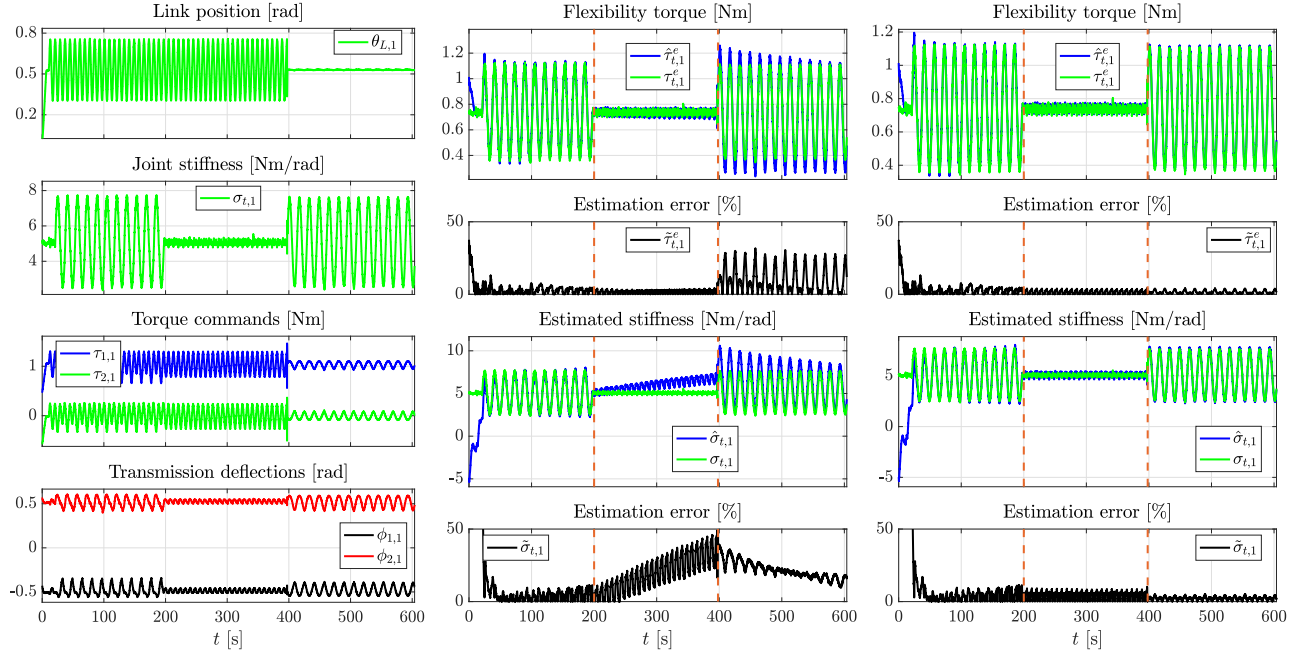


Fig. 4. Experiment #1 (One degree-of-freedom setup) - The left-most column includes the desired link position and joint stiffness, motors' commanded torques and obtained deflections; the mid and right-most columns report the estimated and model-based computed flexibility torques and stiffnesses without and with parameter update termination, respectively.

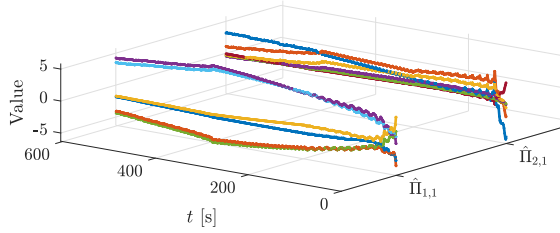


Fig. 5. Experiment #1 (One degree-of-freedom setup) - Temporal evolution of the parameter vectors experimentally estimated via the RLS algorithm without update termination.

TABLE II  
EXPERIMENT #1 - EVALUATION CRITERIA

		MSE [Nm <sup>2</sup> /rad <sup>2</sup> ]	MSREP [%]
With drift	Stiffness	0.5304	0.0187
	Torque	$8.8 \cdot 10^{-6}$	$3.3 \cdot 10^{-5}$
Without drift	Stiffness	0.0258	0.001
	Torque	$1.1 \cdot 10^{-6}$	$2.7 \cdot 10^{-6}$

## V. EXPERIMENTAL VALIDATION

This section presents results of the experimental validation of the proposed approach for stiffness estimation, by using a real soft robot with flexible joints. Joints are actuated by *Qbmove Maker Pro* VSA devices [31], internally driven by two Hitec DC servo motor drives. For each VSA, three magnetic encoders with a resolution of 8192 pulses per revolution measure the position of the two VSA's motors and of the corresponding link, and two current sensors are used to measure motors' currents, thereby indirectly providing accurate information about the achieved motor torque. Reference flexibility

torque and stiffness models are taken from the manufacturer's data-sheet and consists of the ones described in Eq. 9. A sampling rate  $T = 5 \cdot 10^{-3}$  [s] has been adopted.

In order to first prove the validity of our solution, two experiments of increasing complexity have been designed. Both of them include three consecutive test phases: 1) during the first phase (for  $t \in [0, 200)$ ), both link positions and joint stiffnesses are chosen as sinusoids, 2) during the second phase ( $t \in [200, 400)$ ), only link positions are varying and joint stiffnesses are constant, while 3) during the third phase ( $t \in [400, 600)$ ) link positions are constant and joint stiffnesses are required to vary. One of the sought results from the experiments is indeed also the assessment of the method's effectiveness, during different operational conditions. Robots used for e.g. grasping tasks may be required to keep their link positions constant, while varying their joint stiffnesses, while when employed for manipulation they need to guarantee a constant stiffness for changing position. More precisely, the desired position and stiffness signals, during the three phases, are as follows:

$$\begin{aligned} \text{Phase 1: } & \begin{cases} \theta_{L,j}(t) = 0.53 + 0.2 \sin(\pi t/4) \text{ [rad]}, \\ \sigma_{t,j}(t) = 5 + 2.5 \sin(\pi t/8) \text{ [Nm/rad]}; \end{cases} \\ \text{Phase 2: } & \begin{cases} \theta_{L,j}(t) = 0.53 + 0.2 \sin(\pi t/4) \text{ [rad]}, \\ \sigma_{t,j}(t) = 5 \text{ [Nm/rad]}; \end{cases} \\ \text{Phase 3: } & \begin{cases} \theta_{L,j}(t) = 0.53 \text{ [rad]}, \\ \sigma_{t,j}(t) = 5 + 2.5 \sin(\pi t/8) \text{ [Nm/rad]}. \end{cases} \end{aligned}$$

The first experiment has been carried out by using a soft robot with only one degree of freedom, actuated by a single VSA device. Fig. 4 and Fig. 5 report the obtained results. The test reveals that our approach is capable of estimating both flexibility torque and stiffness. It is noticeable that simultaneous position and stiffness variations, which occur

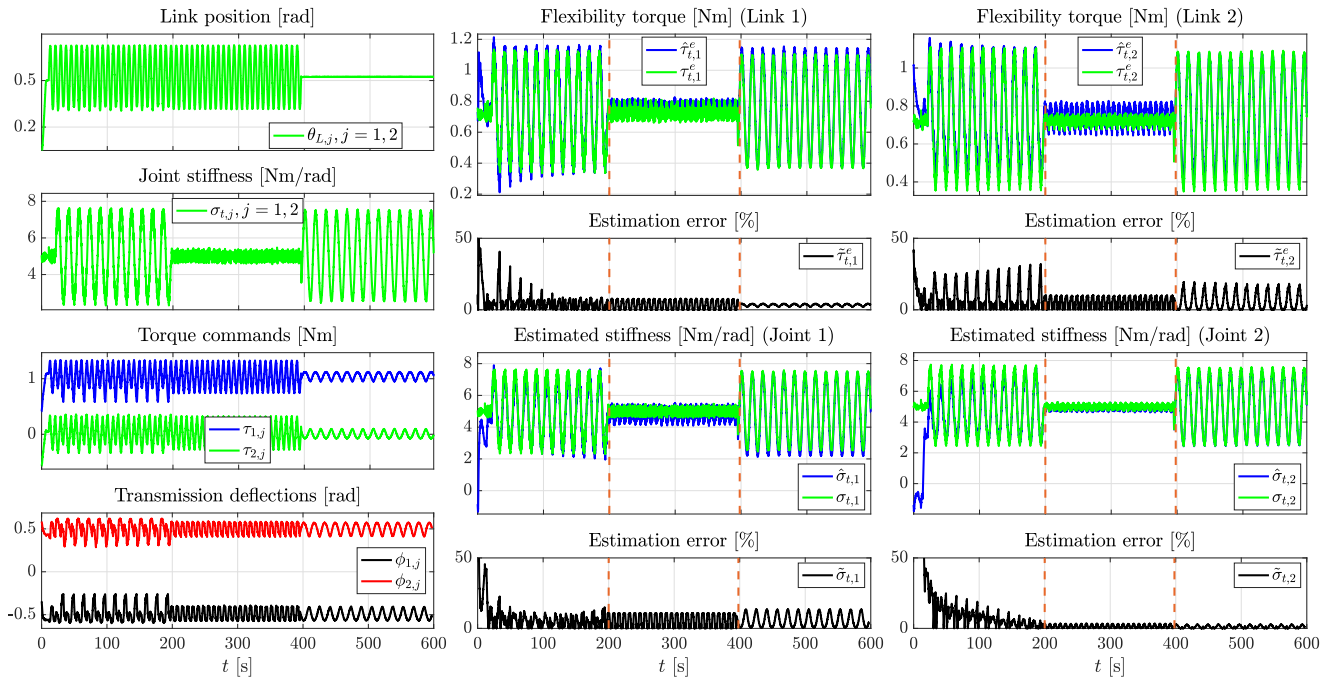


Fig. 6. Experiment #2 (Two degree-of-freedom setup) - The left-most column illustrates desired and commanded quantities for all joints and motors; the mid and right-most column show estimation results for the first and second joint, respectively.

TABLE III  
EXPERIMENT #2 - EVALUATION CRITERIA

	Without drift	MSE [Nm <sup>2</sup> /rad <sup>2</sup> ]	MSREP [%]
Stiffness estimation	1 <sup>st</sup> joint	0.048	0.002
	2 <sup>nd</sup> joint	0.033	0.001
Torque estimation	1 <sup>st</sup> joint	$9 \cdot 10^{-4}$	0.002
	2 <sup>nd</sup> joint	$1.1 \cdot 10^{-5}$	$4 \cdot 10^{-5}$

during the first phase, have a positive overall benefit to the estimation process. Indeed, apart from the initial estimation error of the RLS, due to the imprecise initialization of its parameters, the algorithm itself shows good performance, which only degrades when its input signals (including the transmission deflection  $\phi_i$ ) are poorly exciting. To be more precise, it is known from [19] that, to better estimate the time-varying joint stiffness, it is necessary that the transmission deflection  $\phi_i$  covers larger ranges, so that more information is provided to the estimation process. It is apparent that, during the second phase, the transmission deflection is instead almost constant (refer to the bottom-left plot in Fig. 4), which leads to worse RLS performance, and, consequently, to the observed drift of the stiffness estimation. Furthermore, the estimation performance is improved when the input signal has a richer spectral content. As a rule of thumb [30], given the  $\kappa$  parameters of the RLS, it is advisable to have  $\kappa$  spectral lines in the spectrum of the algorithm's input signal, meaning that the input signal is persistently exciting of order  $\kappa$ . To this respect, by observing frequency domain of the transmission deflection, the richest spectral content of the RLS input is present during the first phase, where indeed it shows its best accuracy. In line with this, if the transmission deflection is

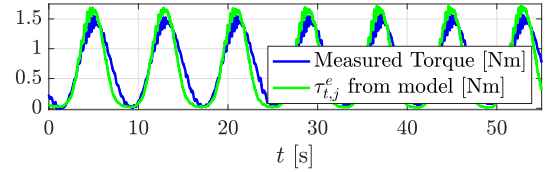


Fig. 7. Torque model validation.

constant or it has poor frequency content with respect to the number of the RLS algorithm parameters, then it presents poor excitation to the RLS algorithm which becomes prone to instability and divergence.

Therefore, a strategy to avoid this limitation and prevent such negative side-effects (including the drift of stiffness estimation in the second phase), is to stop the parameters' update, whenever the poor excitation condition is detected. In our experiment, during the first phase, when the input signal is sufficiently exciting, parameters reach a combination of values allowing an accurate enough estimation of the flexibility torque function, and consequently of the stiffness. This in turn enables good estimation performance even afterward (for  $t > 200$  [s]), when the parameter update is terminated (see the last column of Fig. 4). The corresponding MSE and MSREP criteria are presented in Tab. II.

Capitalizing on the outcomes of the first experiment, a second test has been carried out by using a two degree-of-freedom setup, with the main purpose to experimentally validate the proposed method for multiple link robots with flexible joints. Specifically, results reported in Fig. 6 show that the dynamic coupling between joints does not impact the performance of the flexibility torque and stiffness estimation processes. As for the previous experiment, MSE and MSREP criteria have been calculated and listed in Tab. III.

As a final step towards the method validation, we have verified the accuracy of the sensor model in Eq. 9 by using a force/torque sensor ATI Axia80. Fig. 7 shows the comparison of measured torque and model-based computation of it, during a sinusoidal motion of the link.

## VI. CONCLUSION

The problem of estimating stiffness in flexible robot joints driven by electrical VSAs was addressed in this work. The proposed solution included a delayed UIO, reconstructing flexibility torques at each electrical drive, and an RLS algorithm, subsequently obtaining stiffness from a parameterization of the torque expression with respect to the flexible transmission. Validation via simulation showed that both flexibility torque and stiffness are well estimated, while experimental tests revealed a slow stiffness estimation drift in case of poor excitation. However, as we showed, the problem can be overcome by stopping parameter vector updates when such condition occurs. Moreover, the solution has shown several advantages. First, there are no observability issues, since the problem is tackled from the motor side. Secondly, torque and velocity sensors do not have to be mounted, as the UIO simultaneously estimates the motor's speed and reconstructs the flexibility torque. Third, the observer's matrices are a-priori calculated, making tuning of this method easier than that of state-of-the-art solutions. Fourth, thanks to the decentralized property of motor's dynamics, the proposed solution can be applied to multiple degree-of-freedom articulated soft robots. The main limitation of the method is the need for persistent excitation of the RLS algorithm. However, we are confident that, in the future, more elegant solutions can be found. Future work will extend the research in order to also estimate other relevant impedance parameters.

## VII. ACKNOWLEDGMENTS

The authors wish to thank Nikola Knežević, Branko Lukić, and Predrag Todorov for their help in the experiments.

## REFERENCES

- [1] G. Hirzinger, A. Albu-Schaffer, M. Hahnle, I. Schaefer, and N. Sporer, "On a new generation of torque controlled light-weight robots," in *IEEE Intl. Conference on Robotics and Automation*, vol. 4. IEEE, 2001, pp. 3356–3363.
- [2] C. Della Santina, R. K. Katzschmann, A. Biechi, and D. Rus, "Dynamic control of soft robots interacting with the environment," in *Intl. Conference on Soft Robotics (RoboSoft)*. IEEE, 2018, pp. 46–53.
- [3] C. Della Santina, C. Piazza, G. Grioli, M. G. Catalano, and A. Bicchi, "Toward dexterous manipulation with augmented adaptive synergies: The pisa/iit soft hand 2," *IEEE Transactions on Robotics*, no. 99, pp. 1–16, 2018.
- [4] N. Karavas, A. Ajoudani, N. Tsagarakis, J. Saglia, A. Bicchi, and D. Caldwell, "Tele-impedance based stiffness and motion augmentation for a knee exoskeleton device," in *Intl. Conference on Robotics and Automation*. IEEE, 2013, pp. 2194–2200.
- [5] S. Wolf, G. Grioli, O. Eiberger, W. Friedl, M. Grebenstein, H. Höppner, E. Burdet, D. G. Caldwell, R. Carloni, M. G. Catalano *et al.*, "Variable stiffness actuators: Review on design and components," *IEEE/ASME transactions on mechatronics*, vol. 21, no. 5, pp. 2418–2430, 2016.
- [6] R. Bischoff, J. Kurth, G. Schreiber, R. Koeppel, A. Albu-Schäffer, A. Beyer, O. Eiberger, S. Haddadin, A. Stemmer, G. Grunwald *et al.*, "The kuka-dlr lightweight robot arm—a new reference platform for robotics research and manufacturing," in *ISR 2010 and ROBOTIK 2010*. VDE, 2010, pp. 1–8.
- [7] C. Della Santina, C. Piazza, G. M. Gasparri, M. Bonilla, M. G. Catalano, G. Grioli, M. Garabini, and A. Bicchi, "The quest for natural machine motion: An open platform to fast-prototyping articulated soft robots," *IEEE Robotics & Automation Magazine*, vol. 24, no. 1, pp. 48–56, 2017.
- [8] S. Haddadin, K. Krieger, A. Albu-Schäffer, and T. Lilge, "Exploiting elastic energy storage for "blind" cyclic manipulation: Modeling, stability analysis, control, and experiments for dribbling," *IEEE Transactions on Robotics*, vol. 34, no. 1, pp. 91–112, 2018.
- [9] M. Garabini, A. Passaglia, F. Belo, P. Salaris, and A. Bicchi, "Optimality principles in variable stiffness control: The vsa hammer," in *Intl. Conf. on Intelligent Robots and Systems*. IEEE, 2011, pp. 3770–3775.
- [10] A. De Santis, B. Siciliano, A. De Luca, and A. Bicchi, "An atlas of physical human–robot interaction," *Mechanism and Machine Theory*, vol. 43, no. 3, pp. 253–270, 2008.
- [11] G. Palli, C. Melchiorri, and A. De Luca, "On the feedback linearization of robots with variable joint stiffness," in *2008 IEEE international conference on robotics and automation*. IEEE, 2008, pp. 1753–1759.
- [12] F. Petit, A. Daasch, and A. Albu-Schäffer, "Backstepping control of variable stiffness robots," *IEEE Transactions on Control Systems Technology*, vol. 23, no. 6, pp. 2195–2202, 2015.
- [13] J. K. Mills and A. A. Goldenberg, "Force and position control of manipulators during constrained motion tasks," *IEEE Transactions on Robotics and Automation*, vol. 5, no. 1, pp. 30–46, 1989.
- [14] I. Sardellitti, G. Medrano-Cerda, N. G. Tsagarakis, A. Jafari, and D. G. Caldwell, "A position and stiffness control strategy for variable stiffness actuators," in *Intl. Conference on Robotics and Automation*. IEEE, 2012, pp. 2785–2791.
- [15] M. Ruderman, T. Bertram, and M. Iwasaki, "Modeling, observation, and control of hysteresis torsion in elastic robot joints," *Mechatronics*, vol. 24, no. 5, pp. 407–415, 2014.
- [16] N. Diolaiti, C. Melchiorri, and S. Stramigioli, "Contact impedance estimation for robotic systems," *IEEE Transactions on Robotics*, vol. 21, no. 5, pp. 925–935, 2005.
- [17] G. Grioli and A. Bicchi, "A non-invasive, real-time method for measuring variable stiffness," *Robotics Science and Systems VI*, 2010.
- [18] F. Flacco and A. De Luca, "Stiffness estimation and nonlinear control of robots with variable stiffness actuation," *IFAC Proceedings Volumes*, vol. 44, no. 1, pp. 6872–6879, 2011.
- [19] F. Flacco, A. De Luca, I. Sardellitti, and N. G. Tsagarakis, "On-line estimation of variable stiffness in flexible robot joints," *Intl. Journal of Robotics Research*, vol. 31, no. 13, pp. 1556–1577, 2012.
- [20] T. Ménard, G. Grioli, and A. Bicchi, "A stiffness estimator for agonistic–antagonistic variable-stiffness-actuator devices," *IEEE Transactions on Robotics*, vol. 30, no. 5, pp. 1269–1278, 2014.
- [21] S. Sundaram and C. N. Hadjicostis, "Delayed observers for linear systems with unknown inputs," *IEEE Transactions on Automatic Control*, vol. 52, no. 2, pp. 334–339, 2007.
- [22] —, "Partial state observers for linear systems with unknown inputs," *Automatica*, vol. 44, no. 12, pp. 3126–3132, 2008.
- [23] S. Sundaram, "Lecture notes in fault-tolerant and secure control systems."
- [24] M. E. Valcher, "State observers for discrete-time linear systems with unknown inputs," *IEEE Transactions on Automatic Control*, vol. 44, no. 2, pp. 397–401, 1999.
- [25] A. Saberi, A. A. Stoorvogel, and P. Sannuti, "Exact, almost and optimal input decoupled (delayed) observers," *International Journal of Control*, vol. 73, no. 7, pp. 552–581, 2000.
- [26] A. Albu-Schäffer and A. Bicchi, "Actuators for soft robotics," in *Springer handbook of robotics*, B. Siciliano and O. Khatib, Eds. Springer, 2016, ch. 21, pp. 243–282.
- [27] M. Sain and J. Massey, "Invertibility of linear time-invariant dynamical systems," *IEEE Trans. on automatic control*, vol. 14, no. 2, pp. 141–149, 1969.
- [28] M. Hou and R. J. Patton, "Input observability and input reconstruction," *Automatica*, vol. 34, no. 6, pp. 789–794, 1998.
- [29] J. Kautsky, N. K. Nichols, and P. Van Dooren, "Robust pole assignment in linear state feedback," *International Journal of control*, vol. 41, no. 5, pp. 1129–1155, 1985.
- [30] L. Ljung, "System identification: theory for the user," *PTR Prentice Hall, Upper Saddle River, NJ*, pp. 1–14, 1999.
- [31] "QbMove Maker Pro datasheet," <https://www.qbrobotics.com>, accessed: 2019-09-01.